Reports

A Mantle Plume Initiation Model for the Wrangellia Flood Basalt and Other Oceanic Plateaus

Mark A. Richards, David L. Jones, Robert A. Duncan, Donald J. DePaolo

The vast Wrangellia terrane of Alaska and British Columbia is an accreted oceanic plateau with Triassic strata that contain a 3- to 6-kilometers thick flood basalt, bounded above and below by marine sedimentary rocks. This enormous outpouring of basalt was preceded by rapid uplift and was followed by gradual subsidence of the plateau. The uplift and basalt eruptions occurred in less than ~5 million years, and were not accompanied by significant extension or rifting of the lithosphere. This sequence of events is predicted by a mantle plume initiation, or plume head, model that has recently been developed to explain continental flood volcanism. Evidence suggests that other large oceanic basalt plateaus, such as the Ontong-Java, Kerguelen, and Caribbean, were formed as the initial outbursts of the Louisville Ridge, Kerguelen, and Galapagos hot spots, respectively. Such events may play an important role in the creation and development of both oceanic and continental crust.

The ocean basins contain a number of large basaltic plateaus whose origins are uncertain. Some of the largest of these plateaus may have been erupted rapidly (<5 to 10 million years); if so, they may be the oceanic equivalent of continental flood basalts (*1*). Perhaps the best exposed of these plateaus is Wrangellia, an accreted terrane along the western North American continental margin (*2*). The Triassic section of Wrangellia contains a huge thickness of tholeiitic flood basalt (greenstone) overlying and overlain by marine sedimentary rocks that record the geologic events preceding and following the basalt eruptions. Thus Wrangellia affords an opportunity to study the genesis of an oceanic flood basalt event.

Two models (*3*) have been developed recently to explain continental flood basalt events: (i) "passive" continental rifting over a continuous mantle plume (*4*) and (ii) plume initiation, sometimes accompanied by "active" rifting (*1, 5*) in which melting occurs because of the rise of a large initial diapir or starting plume (Fig. 1) (*6*). The passive model predicts that flood basalt occurrences are restricted to continents and are associated with rifting. The plume initiation model predicts that flood basalts should occur in oceanic as well as continental settings and are not necessarily associated with rifting (*1, 7, 8*).

The plume initiation model also predicts a particular sequence of geologic events. The plume heads, which are as large as ~1000 km in diameter (*5, 9*), melt to produce a flood basalt sequence, and their following feeder conduits (tails) produce associated long-lived hot-spot tracks (*1*). Rapid uplift, of ~1 km, should occur as the plume head rises beneath the lithosphere. The flood basalt eruptions then occur over a short time interval of a few million years and are followed by gradual thermal subsidence of the plateau. The basalts are expected to be tholeiitic and intermediate in composition between depleted mid-ocean ridge basalt (MORB) and enriched ocean island basalt (OIB) (*5, 10*). In this paper we show that these predictions describe the Triassic geology of Wrangellia extremely well. We also review evidence that other oceanic plateaus may represent plume initiation events.

The Wrangellia terrane (*2*) comprises several large allochthonous blocks along the northwest coast of North America between Vancouver Island, British Columbia, and southern Alaska (Fig. 2) (*11*) and is distinguished by its distinctive Triassic strata, consisting of a large thickness of greenstone (basalt) bounded below and above by Middle and Upper Triassic marine sedimentary rocks (Fig. 3). The Triassic rocks lie uncomformably upon a Paleozoic marine sequence that includes island arc complexes whose last activity predates the Triassic basalts by more than 80 million years. Paleomagnetic studies and tectonic reconstructions indicate that the Triassic basalts were erupted at a latitude of about 10° to 17° (*12–15*) in the eastern (*16*) or western Pacific Ocean (*17*) and that Wrangellia was accreted onto the continental margin during the mid-Cretaceous (*18*) or Jurassic (*19*). The huge thickness (up to 6000 m) of basalt, essentially uniform in composition, rapidly erupted, and lying between marine sedimentary formations, has no obvious analogue or explanation in terms of plate boundary volcanism such as island arc formation or sea-floor spreading. Stratigraphic and compositional relations show that the Wrangellian basalts constitute a single flood basalt event (*20*).

The basement rocks are best known in the Wrangell Mountains, Alaska, where they include the Tetelna Volcanics, Slana Spur, and Station Creek Formations and have an aggregate thickness of 2 to 3 km. Widespread plutons yield K-Ar dates of 285 to 297 Ma (million years ago; late Pennsylvanian to earliest Permian) (*21*).

Postarc sedimentary rocks consist of Lower Permian shallow water fossiliferous limestone, sandstone, and shale and, locally, mid- to Upper Permian deep water argillite and radiolarian chert. This stratigraphic sequence indicates that cooling and gradual subsidence followed the cessation of arc volcanism at ~285 Ma. Terminal Permian deposition occurred at depths greater than the calcium carbonate compensation depth (CCD), estimated to be at least 1 km deep at that time, so that the minimum rate of subsidence was ~0.04 mm/year. Permian strata are overlain conformably by a thin (generally <100 m thick) discontinuous unit of black argillite, siltstone, and minor limestone that contains abundant specimens of the Middle Triassic (Ladinian) bivalves *Daonella degeeri* and *D. frami*. This unit also was deposited in deep water (basinal), but probably just above the CCD.

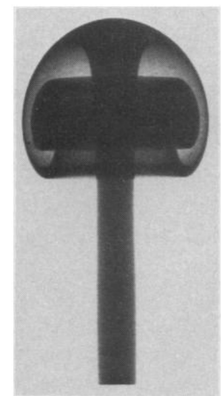

Fig. 1. Photograph of a starting plume produced in one of Griffiths and Campbell's (*34*) laboratory experiments, in which a hot, red-dyed plume was injected at a constant rate at the bottom of a tank of cooler fluid. The darker regions of the plume represent the highest content of original (dyed) plume source material. The lighter regions represent surrounding fluid that has been heated by the plume and thermally entrained into the rising flow. Because the plume material is hot, it has a somewhat lower viscosity than the surrounding fluid, enhancing the contrast between plume head and plume stem diameters.

M. A. Richards, D. L. Jones, D. J. DePaolo, Department of Geology and Geophysics, University of California, Berkeley, CA 94720.
R. A. Duncan, College of Oceanography, Oregon State University, Corvallis, OR 97331.

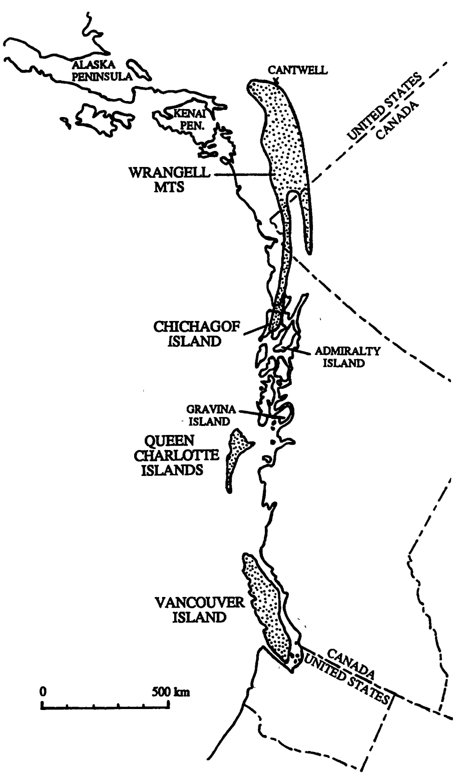

Fig. 2. Regional map (*2*) with stippled areas showing the Wrangellia terrane locations discussed in the text.

The *Daonella* beds are immediately overlain by either subaerial basalt or, locally, by pillowed basalt of the Nikolai Greenstone. The lack of intervening shallow water deposits implies that uplift was rapid. An uplift rate of ~5 mm/year is implied if the *Daonella* beds were deposited at ~500 m water depth and no more than ~1 million year separated deposition of the last *Daonella* bed from extrusion of the basal basalt of the Nikolai. The Nikolai Greenstone reaches a cumulative thickness of >3500 m. Mainly subaerial basaltic volcanism continued throughout most of the Carnian and ceased abruptly toward the end of the late Carnian—a time span of 4 to 5 million years.

Intrusion of large gabbro and diabase sills into Permian and Middle Triassic sedimentary rocks locally accompanied basaltic volcanism (*22*). Dikes are much scarcer than sills throughout Wrangellia, and no sheeted dike complex has been found that would be indicative of crustal extension during volcanism.

With cessation of volcanism, marine sedimentation commenced, first with tidal carbonate rocks (sabhka facies) of the Chitistone Limestone, then through a thick (>1000 m) subsidence assemblage of inner platform carbonate rocks, outer platform carbonate rocks, and finally the basinal limestone and shale of the McCarthy Formation, which contains the Triassic-Jurassic boundary. Initial subsidence rates were about 0.05 mm/year, but this rate soon diminished to about 0.01 mm/year or less. No folding or faulting disrupted stratal continuity for more than 150 million years (*23*) before collision of Wrangellia with North America (*24*).

The upper Paleozoic and Triassic stratigraphy of Vancouver Island is broadly similar to that of Alaska (*2*). This lithic sequence (*25*) is mafic volcanic rocks (Nitinat Tuff), overlain by silicic volcaniclastic rocks (Myra Formation), overlain by an Upper Paleozoic fossiliferous limestone (Butte Lake Formation). The Paleozoic volcanic rocks may be older than those in Alaska, however. Zircons from rocks that intrude the Nitinat Tuff (Tyee Intrusives) yield discordant $^{234}U/^{206}Pb$ ages from 340 to 393 Ma (Mississippian to Early Devonian) (*35*). Zircons from the Myra Formation likewise yield ages greater than 370 Ma (*26*). Volcanism may have at least locally extended into the Permian (*27*).

The Paleozoic rocks of Vancouver Island are overlain by the Karmutsen Formation, which is divided into (*28*) a basal member, over 2500 m thick, composed of pillow lava; a middle member, 600 to 1100 m thick, of pillow breccia and aquagene tuff; and an upper member, up to 3000 m thick, of basalt flows, minor amounts of pillow lava, and some sedimentary layers. The Karmutsen Formation contains a much higher percentage of pillow basalts and aquagene tuffs, indicative of formation under water, than the Nikolai Greenstone of Alaska. However, there are also subaerial flows in the upper part of the Karmutsen (*28*); thus, it appears that most of the eruptions occurred near sea level. Like the Nikolai, the Karmutsen Formation rests locally upon shale containing middle Ladinian *Daonella* fossils (*29*).

The Karmutsen Formation is overlain by carbonate rocks whose age and stratigraphic relations are uncertain (*28, 30, 31*). The lower part of this sequence, the upper Carnian Quatsino Limestone, is a shallow water or carbonate platform deposit (*31*) that grades upward into the overlying Parson Bay Formation. The Parson Bay ranges from late Carnian through Late Triassic in age, and upper Norian faunas, including those containing *Monotis subcircularis*, are found in the higher parts of the formation. These post-Karmutsen formations record gradual subsidence, as do the Chitistone and McCarthy Formations overlying the Nikolai Greenstone in Alaska.

Geochemical data on the Karmutsen basalts offer a possible test of the plume head model (Fig. 4). Plume basalts are distinct from MORBs in having lower ε_{Nd} and higher ε_{Sr} (*32*). The ε_{Nd} of samples from the Karmutsen basalts (*33*) is higher than that of most plume-related basalts. This is expected if the plume head entrained a large amount of MORB source material in the upper mantle during its ascent. If the upper mantle had ε_{Nd} of +10 and an Nd concentration of 0.6 ppm (1 times chondritic), and the plume had an ε_{Nd} of 0 to +5 and an Nd concentration of 1.2 ppm (2 times chondritic), the Karmutsen basalts could have been derived from a plume that entrained 40 to 80% MORB source material in the upper mantle. This amount is compatible with that predicted from laboratory plume models (*34*). Remelting of lithospheric mantle overlying the plume head during an oceanic flood basalt event would also tend to displace the basalt signature toward the MORB field.

Most plume basalts (for example, Hawaiian shield basalts, Icelandic basalts) are tholeiitic but have incompatible element concentrations significantly higher than MORBs. Light rare-earth elements (REEs) are typically moderately enriched in plume basalts relative to chondritic abundances. These characteristics are also generally found in continental flood basalts. Both the Nikolai and Karmutsen basalts are almost entirely tholeiitic (*35*). Major and minor element analyses of the Karmutsen basalts indicate that significant fractionation of olivine, orthopyroxene, clinopyroxene, plagioclase, and spinel (*29*) occurred before eruption. The rocks show a moderate enrichment of light REEs relative to chondritic abundances (*36*), although a small number of samples of the Karmutsen basalts have MORB-like

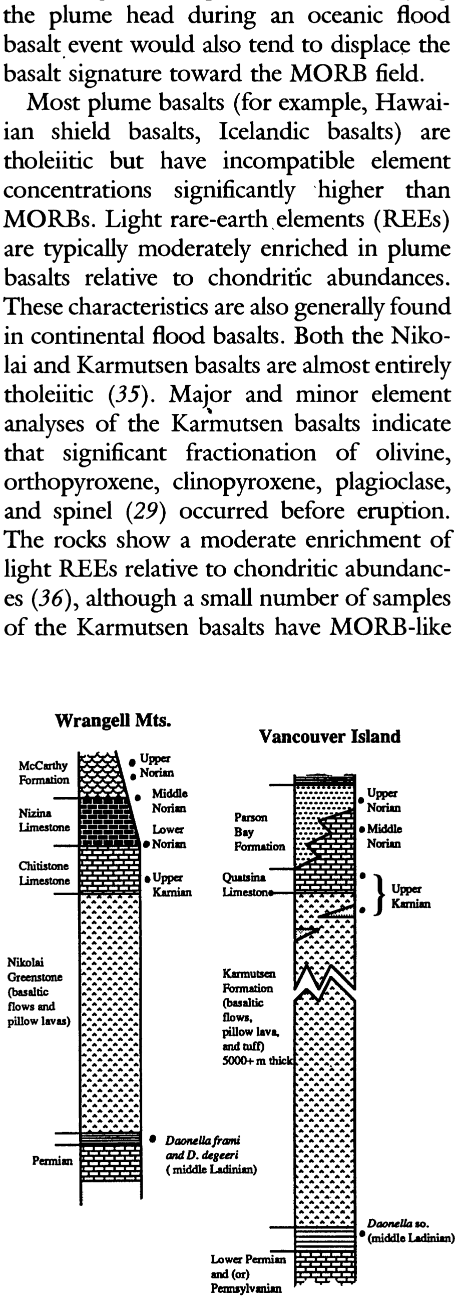

Fig. 3. Diagrammatic stratigraphic columns showing the Triassic rocks of Wrangellia exposed in the Wrangell Mountains and on Vancouver Island. Occurrence of age-diagnostic fossils indicated by black dots.

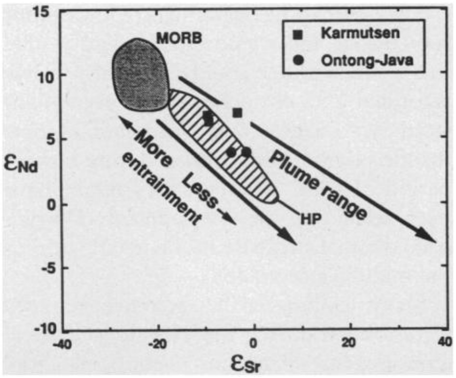

Fig. 4. Nd and Sr isotopic compositions of basalts from the Karmutsen Formation, Vancouver Island (*33*), and from the Ontong-Java plateau (*48*). Fields of MORB and Hawaiian lavas (HP) shown for comparison. Large arrows envelope the compositions of most plume-derived basalts, and small arrows show the effect of entrainment of upper mantle material. Hawaiian data show that any or all of three factors—entrainment efficiency, lithospheric melting, and plume composition—can vary with time; therefore, it may be difficult to fingerprint plumes geochemically. The few Karmutsen and Ontong-Java basalts measured have compostions compatible with a plume origin.

patterns where the light REE are slightly depleted (*29*). Using 11 different plots for major and minor elements, Barker *et al.* (*29*) concluded that the Karmutsen basalts were arc-related. However, in all but one diagram the samples fall largely within or across fields of within-plate basalts and normal or enriched MORBs. Although some samples fall in the arc fields, there is no overall basis for ruling out a plume origin.

In summary, the major and minor element compositions and the isotopic compositions of the Triassic Wrangellian basalts are consistent with a plume origin. They tend to be transitional between MORB and typical within-plate basalts associated with established plumes, both in terms of chemistry and isotopic compositions, as is expected if they were derived from partial melting of a plume head.

We seek to explain the origin of the Nikolai and Karmutsen basalts on the basis of the stratigraphic and geochemical data summarized above. A synthesis of the geological history of Wrangellia is shown in Fig. 5. The phase of rapid uplift followed by flood volcanism is difficult to explain in terms of normal island arc activity. Earlier suggestions share the common attribute of rifting of either the Paleozoic island arc complex or rifting of an adjacent, contemporaneous island arc (the Wallowa terrane) (*29, 33*), in analogy to the post-Miocene tectonic evolution of the Marianas volcanic arc and back-arc rift system. However, such models are inadequate in a number of respects. First, there is no compelling evidence for large amounts of crustal extension and graben formation (normal faulting) or even significant tilting in the older sedimentary strata. Instead, the basalt flows appear to be nearly flat-lying and are conformable with the underlying sedimentary rocks. Second, the widespread emplacement of gabbroic sills and the lack of sheeted dike complexes also implies that the crust did not undergo significant extension during the eruptions (although minor extension must have occurred in order for the basalt to have been erupted through the crust). Third, during rifting of an arc one would expect subsidence and submarine volcanism at depths comparable, perhaps, to those of mid-ocean ridges. Instead, the basalts are largely subaerial or shallow submarine basalts. Fourth, the Paleozoic island arc complex underlying much of Wrangellia was ~100 million years old at the time of the basalt eruptions, unlike in the Marianas, where a young arc was rifted (*37*). An alternative model involving rifting of an adjacent, active arc (*29*) does not explain evidence (sills and dikes) that the Nikolai and Karmutsen basalts were erupted through the underlying sedimentary rocks.

We propose that a large hot diapir of deep mantle material, a starting plume, rose beneath the oceanic lithosphere, which happened in this case to have been an old island arc complex. Rapid uplift of the ocean floor preceded the sudden onset of a huge partial melting event involving both deep (enriched) mantle and thermally entrained (depleted) upper mantle material (see Fig. 1) as well as, perhaps, preexisting oceanic lithosphere and island arc crustal material. During melting the oceanic Moho may have acted as a density filter, resulting in eruption of almost purely tholeiitic lavas produced by crystal fractionation from a more picritic melt (picrites are only present locally as ultramafic cumulates associated with the gabbroic sill complexes). Gradual thermal subsidence of the lithosphere followed the abrupt termination of basaltic volcanism. The presence of thickened crust (arc volcanics, sediments, and flood basalt) as well as, perhaps, an underlying lithosphere of highly refractory residual material made this province difficult to subduct. Rather, it was accreted onto the continental margin of North America.

The plume initiation model for Wrangellia may apply to other large oceanic plateaus. The Kerguelen and Ontong-Java plateaus are the two largest oceanic plateaus. The Kerguelen plateau appears to be basaltic (*38*) and to have formed between 110 and 115 Ma at the present-day location of the Kerguelen hot spot (*39–41*). The Rajmahal Traps of eastern India also formed at the Kerguelen hot spot at ~117 Ma (*42*). Plate motions have juxtaposed the older Kerguelen plateau again against the active hot spot, so that the smaller northwest part of the plateau represents recent hot spot activity. Davies *et al.* (*40*) suggested that even earlier activity of the hot spot may be marked by the 135-million-year-old Bunbury basalt in southwestern Australia and the ~124-million-year-old Naturaliste plateau; however, recent plate reconstructions (*43*) do not support these associations.

Geochemical studies (*38, 44*) suggest that the plateau basalts were produced by melting of an enriched OIB-type source contaminated by a depleted MORB-type source and components derived from continental lithosphere (*45*), as expected in a rising plume head (*34*) (Fig. 1). The volume of basalt in the older part (115 Ma) of the Kerguelen plateau could be as much as 10 million km^3 (*40*), and the crust under both plateaus may be thicker than normal (*46*).

The mid-Cretaceous Ontong-Java plateau has been postulated to have formed, as has Iceland, at an on-ridge hot spot over a period of ~50 million years or more (*47*) or as a flood basalt associated with a plume head at the beginning of the Louisville hot spot track (*1*). Geochemical data from the Ontong-Java (and Manihiki) plateaus are consistent with either of these models (*48, 49*).

Analyses of drill cores of the bottommost sediments overlying the basaltic basement suggest that the Ontong-Java plateau formed at about 120 Ma (*50*); ^{40}Ar-^{39}Ar dating of a basalt sample from the island of Malaita, possibly an obducted fragment of the margin of the Ontong-Java plateau [but see (*51*)], also yields an age of about 120 Ma

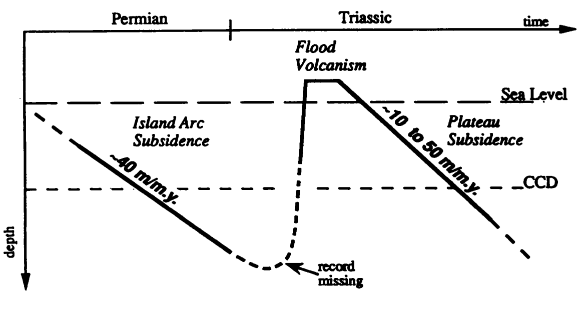

Fig. 5. Schematic subsidence and uplift history of Wrangellia as deduced from analysis of the strata (fossil ages) underlying and overlying the Nikolai and Karmutsen greenstones; m.y., million years.

(*8*). Multiple ^{40}Ar-^{39}Ar incremental heating dates from older DSDP (Deep-Sea Drilling Program) basement samples (site 289) and from ODP (ocean-drilling program) samples (site 807) on the high central plateau yield ages of 120 to 124 Ma (*52*). Tarduno *et al.* (*53*) also argued from paleomagnetic and stratigraphic evidence that the entire plateau formed in a brief portion of the early Aptian between ~121 and 124 Ma. Basalts from sites 289 and 807 show similar major and trace element as well as isotopic geochemical signatures (*48, 54*). These data suggest that the bulk of the Ontong-Java plateau basalts were erupted very rapidly at about 120 to 125 Ma, consistent with the plume head model.

Much of the Caribbean plate has long been recognized as anomalously shallow and thick (*55, 56*). Multichannel seismic reflection profiles suggest that the western Colombian Basin is an oceanic plateau formed by basalts extruded onto preexisting oceanic crust (*57*). This group of basalts also includes formations throughout the Greater Antilles, along the northern coast of South America from Trinidad to the Guajira Peninsula of Columbia, and along the Pacific margin from central Guatemala south to Ecuador, in addition to the basinal basalts (*59*).

Most radiometric dates on the Caribbean basalts are Late Cretaceous, between about 80 and 90 Ma. The top of the basalt horizon ranges from latest Turonian in the Venezuelan Basin (DSDP sites 146, 150, and 153) to early Campanian on the lower Nicaraguan Rise (site 152) (*58*). Basaltic eruptions thus appear to have terminated at ~80 Ma over a broad area. Exposures show mostly pillow basalts [including picrites and komatiites (*60*)] interlayered with marine and terrigenous sedimentary rocks; mafic and silicic intrusive bodies are also found. Many of these formations are thought to have been emplaced as allochthonous blocks or thrust sheets (for example, in Venezuela and Columbia), perhaps similar to the emplacement of Wrangellia. Basalt thicknesses range as high as 9 km in a number of locations (*59*). In at least one case (the Villa de Çura Nappe in Venezuela), basaltic volcanism appears to have been preceded by uplift.

Although the Late Cretaceous basalts of the Caribbean are oceanic and have been classed as ophiolites, they do not represent normal mid-ocean ridge activity. These rocks have both mid-ocean ridge (MORB) and ocean island (OIB) affinities (*59*). The total volume of anomalously thick basaltic crust emplaced is at least several million cubic kilometers. Plate tectonic reconstructions for the Caribbean region (*61*) show that a stationary Galapagos plume would have been located beneath the Venezuelen basin at about the time of these voluminous eruptions and that the Caribbean Basalt Province may have been the result of the initiation of the Galapagos hot spot (*1*).

In order to understand better the genesis of these huge oceanic basalt plateaus, aspects of the plume head model need to be investigated further. Although it is plausible that sublithospheric partial melting in a rising plume head ~600 to 1000 km in diameter and ~100° to 250°C hotter than ambient mantle is sufficient to generate the large areal extent and erupted volumes of continental flood basalts and oceanic plateaus (*1, 5, 62, 63*), we lack dynamical models combining the physics of solid-state convection and melt extraction as a plume head encounters the lithosphere. It is unclear how such a huge volume of mantle source material can move through a shallow melting region in just a few million years. Small-scale convection within the flattening plume head may be important (*64*). Similarly, we lack models for the uplift history and tectonic response of the lithosphere during a plume head melting event.

Certain aspects of Wrangellian geology may provide unique constraints on models of flood basalt petrogenesis. The duration of uplift and volcanism (<5 million years) show that flood basalt events occur rapidly. The short duration of precursory uplift and flood basalt eruption in Wrangellia, along with the age (~100 million years) of the preexisting lithosphere, have another important implication. In the absence of extension, significant thinning of the lithosphere could not have occurred quickly; consequently, melting temperatures and depths must have been somewhat greater than those advocated by either White and McKenzie (*4*) or Griffiths and Campbell (*5*). We suggest that the Wrangellian flood basalt resulted from melting of a plume head at least ~250°C hotter than ambient mantle at depths of ~70 to 200 km (*63*).

Wrangellia may differ in one important way from other oceanic plateaus: The Triassic basalts of Wrangellia make up only part of the total crustal section, whereas almost the entire crustal section of some major oceanic plateaus may form during single flood basalt events. It is possible that pieces of Wrangellia were accreted (as opposed to subducted) only because the flood basalts overlay a thick section of island arc crust, and that oceanic plateaus are more typically subducted.

Our model for oceanic plateaus contrasts to Larson's (*65*) suggestion that the mid-(and Late) Cretaceous oceanic plateaus and continental flood basalts were caused by a single "superplume." Some of these basaltic events occur at the beginnings of known hot spot tracks, and we consider it implausible that a single plume could cause such widely separated and distinct eruptive events. Instead, we suggest that a number of new mantle plumes were formed during a short period of time, although they might have been related to the development of large-scale thermal structure in the mantle during the mid-Cretaceous (*66*).

Many circum-Pacific accreted terranes were formed during the Triassic, and these terranes generally contain major basaltic formations. It seems likely that some of these accreted terranes are remnants of oceanic plateau flood basalt events. Both the Triassic and Cretaceous basaltic flare-ups correspond to periods of major continental breakup; this observation suggests that mantle plume initiation events may have an important, perhaps episodic, role in Earth history.

REFERENCES AND NOTES

1. M. A. Richards, R. A. Duncan, V. E. Courtillot, *Science* **246**, 103 (1989).
2. D. L. Jones, N. J. Silberling, J. Hillhouse, *Can. J. Earth Sci.* **14**, 2565 (1977).
3. W. J. Morgan, in *The Sea*, C. Emiliani, Ed. (Wiley, New York, 1981), vol. 7, pp. 443–475.
4. R. S. White and D. P. McKenzie, *J. Geophys. Res.* **94**, 7685 (1989).
5. I. H. Campbell and R. W. Griffiths, *Earth Planet. Sci. Lett.* **99**, 79 (1990).
6. See also, J. A. Whitehead and D. S. Luther, *J. Geophys. Res.* **80**, 705 (1975); P. Olson and I. S. Nam, *ibid.* **91**, 7181 (1986).
7. P. R. Hooper, *Nature* **345**, 246 (1990).
8. R. A. Duncan and M. A. Richards, *Rev. Geophys.* **29**, 31 (1991).
9. P. Olson, G. Schubert, C. Anderson, *J. Geophys. Res.*, in press.
10. R. W. Griffiths, *J. Fluid Mech.* **166**, 115 (1986); M. A. Richards and R. W. Griffiths, *Nature* **342**, 900 (1989).
11. We do not include the Wallowa terrane of Oregon in our strict definition of the Wrangellia terrane because the calc-alkaline nature of the Triassic volcanic rocks makes such an association uncertain.
12. J. W. Hillhouse, *Can. J. Earth Sci.* **14**, 2578 (1977).
13. R. W. Yole and E. Irving, *ibid.* **17**, 1210 (1980).
14. J. W. Hillhouse, C. S. Gromme, T. L. Vallier, *J. Geophys. Res.* **87**, 3777 (1982).
15. J. W. Hillhouse and C. S. Gromme, *ibid.* **89**, 4461 (1984).
16. C. R. Newton, *U.S. Geol. Surv. Prof. Pap. 1435* (1986).
17. D. C. Engebretson, A. Cox, R. G. Gordon, *Geol. Soc. Am. Spec. Pap.* **206**, 1 (1985).
18. J. W. H. Monger *et al.*, *Geology* **10**, 70 (1982).
19. P. Van der Heyden, *Geol. Surv. Can. Pap. 91-1A* (1991), p. 79.
20. B. C. Panuska, *Geol. Soc. Am. Abstr. Progr.* **22**, A168 (1990).
21. H. C. Berg, D. L. Jones, D. H. Richter, *U.S. Geol. Surv. Prof. Pap. 800-D* (1972), p. D1.
22. W. J. Nockelberg, D. L. Jones, N. J. Silberling, *Geol. Soc. Am. Bull.* **96**, 1251 (1985).
23. There is, however, some evidence for Jurassic deformation at the margins of the Vancouver Island part of the terrane [J. W. H. Monger, *Geol. Surv. Can. Pap. 91-1A*, 219 (1991)].
24. D. L. Jones, N. J. Silberling, J. Hillhouse, *Geol. Soc. Am. Spec. Publ.* **19**, 367 (1976).
25. J. E. Muller, *Geol. Surv. Can. Pap. 79-30* (1980), p. 1; *Can. J. Earth Sci.* **14**, 2062 (1977); M. T. Brandon *et al.*, *Geol. Surv. Can. Pap. 86-1A* (1986), p. 683.
26. A pre-Mississippian age for the Nitinat Tuff is also

supported by the presence of Lower Mississippean conodonts in chert and tuff that may overlie unconformably the Nitinat tuff.
27. R. W. Yole, *Proc. Geol. Assoc. Can.* **20**, 30 (1969).
28. J. E. Muller, K. E. Northcote, D. Carlisle, *Geol. Surv. Can. Pap. 74-8* (1974), p. 1.
29. F. Barker, A. S. Brown, J. R. Budahn, G. Plafker, *Chem. Geol.* **75**, 81 (1989).
30. J. A. Jeletzky, *Geol. Surv. Can. Pap. 69-14* (1970), p. 1.
31. E. Carlisle and T. Susuki, *Can. J. Earth Sci.* **11**, 254 (1974).
32. $\varepsilon_{Nd} = 10^4[(^{143}Nd/^{144}Nd_{sample})/(^{143}Nd/^{144}Nd_{CHUR}) - 1]$ where CHUR is the chondritic uniform reservoir. See D. J. DePaolo, *Neodymium Isotope Geochemistry* (Springer-Verlag, New York, 1988). ε_{Sr} is the similar notation for the $^{87}Sr/^{86}Sr$ ratio.
33. S. D. Samson, P. J. Patchett, G. E. Gehrels, R. G. Anderson, *J. Geol.*, in press.
34. R. W. Griffiths and I. H. Campbell, *Earth Planet. Sci. Lett.* **99**, 66 (1990).
35. E. M. MacKevett, Jr., and D. H. Richter, *Geol. Assoc. Can. Cordilleran Sect. Progr. Abstr.* **xx**, 13 (1974).
36. A. Davis and G. Plafker, *Can. J. Earth Sci.* **22**, 183 (1985).
37. J. W. Hawkins and J. T. Melchior, *J. Geophys. Res.* **90**, 11431 (1985).
38. D. Weiss, Y. Bassias, I. Gautier, J.-P. Mennessier, *Geochim. Cosmochim. Acta* **53**, 2125 (1989).
39. Y. Bassias, H. L. Davies, L. Leclaire, D. Weis, *Bull. Mus. Natl. Hist. Nat. Paris* **4/9**, 367 (1987); L. Leclaire *et al.*, *Geo-Marine Lett.* **7**, 169 (1987).
40. H. L. Davies *et al.*, *Contrib. Mineral. Petrol.* **103**, 457 (1989).
41. R. A. Duncan, *J. Volcanol. Geotherm. Res.* **4**, 283 (1978); R. Duncan, unpublished data; H. Whitechurch, R. Montigny, J. Sevigny, M. Storey, V. Salters, *Proc. ODP Sci. Results 120*, in press.
42. A. K. Baksi, *Chem. Geol.* **70**, 46 (1986).
43. J.-Y. Royer and M. F. Coffin, *Proc. ODP Sci. Results 120*, in press.
44. D. Weiss and F. A. Frey, *Eos* **71**, 657 (1990).
45. C. Alibert, *Proc. ODP Sci. Results 119* (1991), p. 293; M. Storey *et al.*, *Proc. ODP Sci. Results 120*, in press.
46. M. Recq and P. Charvis, *Geophys. J. Roy. Astron. Soc.* **84**, 529 (1986); M. Recq, D. Brefort, J. Malod, J.-L. Veinante, *Tectonophysics* **182**, 227 (1990); D. M. Hussong, L. K. Wipperman, L. W. Kroenke, *J. Geophys. Res.* **84**, 6003 (1979).
47. L. W. Kroenke, *Haw. Inst. Geophys. Rep. 72-5* (Univ. of Hawaii, Honolulu, 1972); J. J. Mahoney, in *Seamounts, Islands, and Atolls, AGU Monogr. 43*, B. H. Keating, P. Fryer, R. Batiza, G. W. Boehlert, Eds. (American Geophysical Union, Washington, D.C., 1987), pp. 207–220; The preexisting oceanic lithosphere could not have been more than about 50 million years old at the time of plateau eruption [R. L. Larson, S. M. Smith, and C. G. Chase, *Earth Planet. Sci. Lett.* **15**, 315 (1972).
48. J. J. Mahoney and K. J. Spencer, *Earth Planet. Sci. Lett.*, in press.
49. It has also been postulated that the plateau was principally continental [R. L. Carlson, N. I. Christensen, R. P. Moore, *Earth Planet. Sci. Lett.* **51**, 171 (1980); A. Nur and Z. Ben-Avraham, *J. Geophys. Res.* **87**, 3644 (1982)] but recent geochemical studies do not support this hypothesis (*48*).
50. J. E. Andrews *et al.* (shipboard scientific party), *Init. Rep. Deep Sea Drilling Proj.* **30**, 27 (1975).
51. R. J. Musgrave [*Tectonics* **9**, 735 (1990)] argued on the basis of magnetostratigraphic data that Malaita was not formed as part of the Ontong-Java plateau.
52. R. Duncan, unpublished data.
53. J. A. Tarduno, W. V. Sliter, H. Mayer, paper presented at the Caltech Plume Symposium, Pasadena, CA, May 1991; J. Tarduno, unpublished manuscript.
54. J. Mahoney, personal communication.
55. C. B. Officer, J. I. Ewing, R. S. Edwards, H. R. Johnson, *Geol. Soc. Am. Bull.* **68**, 359 (1957).
56. J. B. Diebold, P. L. Stoffa, P. Buhl, M. Truchan, *J. Geophys. Res.* **86**, 7901 (1981).
57. C. L. Bowland and E. Rosencrantz, *Geol. Soc. Am. Bull.* **100**, 534 (1988).
58. T. W. Donnelly, K. Melson, R. Kay, J. J. W. Rogers, *Init. Rep. Deep Sea Drilling Proj.* **15**, 989 (1973).
59. T. W. Donnelly *et al.*, in *The Geology of North America*, vol. H, *The Caribbean Region*, (Geological Society of America, Washington, DC, 1990), pp. 339–374.
60. M. Storey *et al.*, *Geology* **19**, 376 (1991); L. M. Echeverria, *Contrib. Minaral. Petrol.* **73**, 253 (1980).
61. R. A. Duncan and R. B. Hargraves, *Geol. Soc. Am. Mem.* **162**, 81 (1984).
62. E. M. Klein and C. H. Langmuir, *J. Geophys. Res.* **92**, 8089 (1987).
63. D. P. McKenzie and M. J. Bickle, *J. Petrol.* **29**, 625 (1988).
64. R. W. Griffiths and I. H. Campbell, *J. Geophys. Res.*, in press.
65. R. L. Larson, *Geology* **19**, 547 (1991).
66. M. A. Richards and D. C. Engebretson, *Eos* **71**, 1575 (1990).
67. We thank N. Sleep, M. Coffin, J. Mahoney, N. Donnelly and two anonymous reviewers for helpful comments on the manuscript. Some of the ideas in this paper were developed over the past few years with R. Griffiths, I. Campbell, G. Davies, and R. Hill. We thank R. Griffiths for providing the photograph in Fig. 1.

22 February 1991; accepted 23 July 1991

The DNA Binding Arm of λ Repressor: Critical Contacts from a Flexible Region

NEIL D. CLARKE,* LESA J. BEAMER,† HARRY R. GOLDBERG, CAROL BERKOWER, CARL O. PABO‡

Segments of protein that do not adopt a well-ordered conformation in the absence of DNA can still contribute to site-specific recognition of DNA. The first six residues (NH_2-Ser^1-Thr^2-Lys^3-Lys^4-Lys^5-Pro^6-) of phage λ repressor are flexible but are important for site-specific binding. Low-temperature x-ray crystallography and codon-directed saturation mutagenesis were used to study the role of this segment. All of the functional sequences have the form [X]^1-[X]^2-[Lys or Arg]^3-[Lys]^4-[Lys or Arg]^5-[X]^6. A high-resolution (1.8 angstrom) crystal structure shows that Lys^3 and Lys^4 each make multiple hydrogen bonds with guanines and that Lys^5 interacts with the phosphate backbone. The symmetry of the complex breaks down near the center of the site, and these results suggest a revision in the traditional alignment of the six λ operator sites.

ALTHOUGH THE WELL-CHARACTERized DNA binding motifs (helix-turn-helix, zinc finger, and so forth) use stably folded units of secondary structure for recognition, flexible regions can also contribute to site-specific recognition. Unfortunately, crystallographic studies of such segments are difficult because residual disorder in these segments may result in a poor electron density map. In order to address these problems in studying a flexible DNA-binding segment of λ repressor, we (i) determined the crystal structure of the repressor-operator complex at low temperature to reduce thermal motion and (ii) performed an exhaustive genetic and biochemical analysis to test the functional relevance of the observed crystal structure.

We have focused on the first six residues of λ repressor. This segment has been referred to as an "arm" because of the way it wraps around the operator DNA (see Fig. 1). Nuclear magnetic resonance (NMR) experiments clearly show that this segment is flexible in solution (*1*). Previous crystallographic studies of the protein by itself or of the protein bound to DNA showed only weak electron density for the arm (*2, 3*). However, despite its inherent flexibility, the arm plays a critical role in DNA binding and deletion of the arm results in a greater than 8000-fold reduction in DNA binding affinity (*4*).

The NH_2-terminal arm of λ repressor has the sequence (NH_2-Ser^1-Thr^2-Lys^3-Lys^4-Lys^5-Pro^6-). In order to understand how this segment contributes to DNA binding, we first tested the functional significance of each residue. In separate experiments, each codon in the arm was randomly mutated by oligonucleotide cassette mutagenesis of a plasmid-borne gene encoding the amino-terminal domain of λ repressor (*5*). Subsequent transformation into *Escherichia coli* and selection for resistance to phage infection allowed us to identify a large number of functional sequence variants in the

N. D. Clarke, Howard Hughes Medical Institute and Department of Molecular Biology and Genetics, Johns Hopkins University School of Medicine, Baltimore, MD 21205.
L. J. Beamer and C. Berkower, Department of Molecular Biology and Genetics, Johns Hopkins University School of Medicine, Baltimore, MD 21205.
H. R. Goldberg, Department of Biophysics and Biophysical Chemistry, Johns Hopkins University School of Medicine, Baltimore, MD 21205.
C. O. Pabo, Howard Hughes Medical Institute and Departments of Molecular Biology and Genetics and of Biophysics and Biophysical Chemistry, Johns Hopkins University School of Medicine, Baltimore, MD 21205.

*Present address: Center for Advanced Research in Biotechnology, National Institute of Standards and Technology, Rockville, MD 20850.
†Present address: Molecular Biology Institute, University of California, Los Angeles, CA 90024.
‡Present address: Department of Biology, Massachusetts Institute of Technology, Cambridge, MA 02139.